Systematic analysis of microfluidic probe design and operation

Thomas Gervais, Mohammadali Safavieh, Mohammad A. Qasaimeh, and David Juncker

Abstract— **Microfluidic probes are an emerging tool used in a wide range of applications including surface biopatterning, immunohistology, and cell migration studies. They control flow above a surface by simultaneously injecting and aspirating fluids from a pen-like structure positioned a few tens of microns above a surface. Rather than confining flows inside microchannels they rely on recirculating flow patterns between the probe tip and the substrate to create a hydrodynamic flow confinement (HFC) zone in which reagents can be locally delivered to the surface. In this paper, we provide a theoretical model, supported by numerical simulations and experimental data, describing the extent of the HFC as a function of the two most important probe operation parameters, the ratio of aspiration to injection flow rate, and the distance between probe apertures. Two types of probes are studied: two-aperture microfluidic probes (MFPs) and microfluidic quadrupoles (MQs). In both cases, the model yields very accurate results and suggests a simple underlying theory based on 2D potential flows to understand probe operation. We further highlight how the model can be used to precisely control the probe's "brush stroke" while in surface patterning mode. The understanding of probe operation made possible through the provided analytical model should lay the bases for computer-controlled probe calibration and operation.**

I. INTRODUCTION

Microfluidics traditionally deals with moving fluids into tiny channels to speed up, integrate and automate biochemical sample analysis [1]. Yet, in recent years, there is a growing interest in open microfluidics systems [2], i.e. configurations which still use the basic fabrication material and unique physical behavior of fluids in channel-based microfluidics (low Reynolds number flows, fast diffusion and reaction times, etc.) to control flows in an open, channel-less microfluidic configuration. Thus they can control flow directly on conventional labware such as petri dishes or microscope slides without the use of channels. Most prominent examples are probe-based designs in which flow is introduced by two point openings located on the tip of a pen-like structure (a microfluidic probe or MFP). The probe is brought into close proximity with an immersed surface and the flow is contained in the volume enclosed between the surface to be analyzed and the flat tip of the probe [3]. These probes are used in an increasing number of applications, including biopatterning surfaces [4], analyze biological tissue samples [5,6], perform single cell analysis on a petri dish [7], generate floating concentration gradients [8], and study neutrophil dynamics during chemotaxis under stationary and moving concentration gradients of chemokines [9].

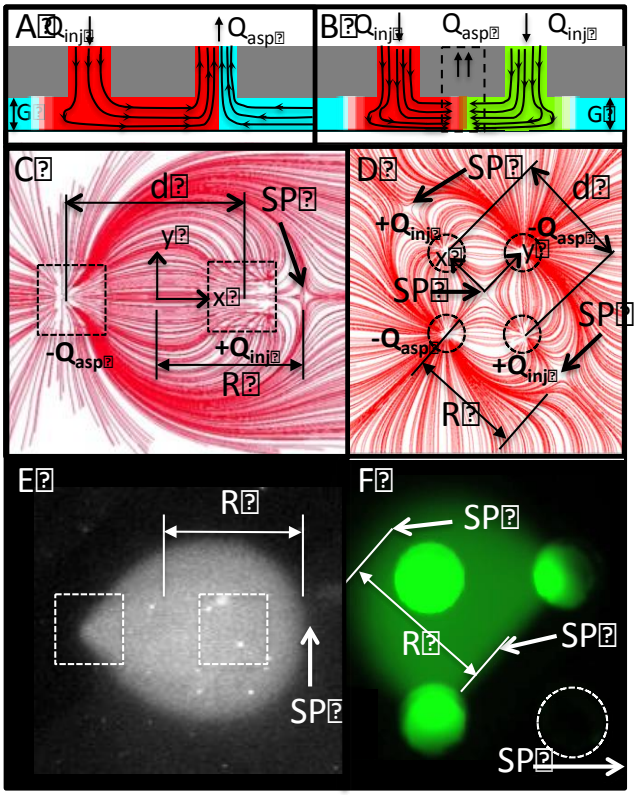

Figure 1. Flow and diffusive transport patterns typically generated by microfluidic multipolar probes. Left: Two-aperture probe (MFP). Right: Four-aperture probe (MQ). A-B: side view of the flow profile in microfluidic probes. C-D: Streamlines view of the flow profile highlighting the presence of a hydrodynamic confinement area and the presence of stagnation points in both cases. Simulation performed using the software COMSOL Inc. (Burlington, MA). E-F: Experimental observation of HFC and diffusion broadening inside flow dipoles and quadrupoles, using E: adsorbed FITC-conjugated IgG[4] and F: Free flowing FITC[8].

Despite their varied applications, MFPs are part of an even larger class of open microfluidic systems that generate flow patterns in a thin quasi 2D gap formed between the

*Research supported by NSERC and FRQNT

Prof. T. Gervais (to whom correspondence should be addressed) is with École Polytechnique de Montréal, QC, Canada (Thomas.Gervais@polymtl.ca, phone: 514-340-4711 ext 3752).

M. Safavieh is with the Institut National de la Recherche Scientifique (INRS), Varennes, QC, Canada (safavieh@emt.inrs.ca).

Prof. M. A. Qasaimeh is with New York University in Abu Dhabi, United Arab Emirates (Mohammad.Qasaimeh@nyu.edu)

Prof. D. Juncker, is with McGill University and Centre d'innovation Génome Québec, Montreal, QC, Canada (David.Juncker@mcgill.ca).

surface to analyze and the tip of the probe, the latter being composed of a flat mesa, often made of etched silicon or poly(dimethylsiloxane), perforated by two or more injection or aspiration apertures [3]. When the gap is narrow compared to the probe mesa surface, a Hele-Shaw flow configuration arises in which flow can be considered irrotational [10]. When the MFP is immersed with the surrounding medium that is covering the bottom substrate, and by aspirating fluid at a rate a few times more than what is injected inside the gap, delivered reagents is fully confined in the vicinity of the probe, in a zone we call the hydrodynamic flow confinement (HFC) area. Because reagents also diffuse from the injected stream to the surrounding medium, the perimeter of the HFC area is blurred due to diffusion broadening of the HFC. This blurring can either be an inconvenience, e.g. when precisely patterning a surface, or an asset to create complex sharp concentration gradients that can be quickly modulated and moved around over a surface by displacing the probe.

In all cases, knowing the geometry of the HFC is of prime importance to accurately operate MFPs either in surface patterning or gradient generation. Several attempts at modeling microfluidic probes have been made in the past, including by our group. Qasaimeh et al. (our group) has shown that flow patterns in a microfluidic quadrupole (MQ) – 4 flow apertures arranged in a square configuration – closely resembles field lines in a two-dimensional electrostatic quadrupole [8]. Further analysis revealed that advective-diffusive behavior can accurately be modeled inside a microfluidic quadrupole using a simple 1D diffusion model. Christ et al. [11] have tackled numerical modeling of flow profiles in MFP and focused on measuring hydrodynamic pressure inside the HFC and simulating the HFC envelope width.

In this paper, we use analytical models and numerical simulations using COMSOL Inc. (Burlington, MA) to extend both analyses and highlight a few key features shared by both MFPs and MQs. We provide the basic framework to model these systems analytically and derive useful scaling laws for both MFPs and MQs. Scaling laws are further confirmed by numerical results and previously published experimental data. The goal of this analysis is to relate the operation and design parameters to precisely control the size and dimension of the HFC.

Table 1: Mathematical analogy between electric and fluidic 2D irrotational fields

	Electrostatics (charge q)	**Electrokinetics** (current I)	**Fluid Mechanics** (flow rate Q)
Scalar Potential	Electrostatic potential $\phi(x,y)$	Electrostatic potential $\phi(x,y)$	Velocity potential $\phi(x,y) = -\frac{G^2 p(x,y)}{12\eta}$
Associated field	Electric field $\mathbf{E} = -\nabla\phi$	Current Density $\mathbf{J} = -\sigma\nabla\phi$	Velocity profile $\mathbf{v} = \nabla\phi$
Gauss's law (continuity equation)	$\oint_S \vec{E}\cdot d\vec{S} = \frac{q}{\varepsilon_0}$	$\oint_S \vec{J}\cdot d\vec{S} = \frac{dq}{dt} = I$	$\oint_S \vec{v}\cdot d\vec{S} = Q$

II. THEORY

A. Hele-Shaw flows and problem formulation

Hele-Shaw flows are special kind of flows, akin to Darcy flows, occurring when a fluid is confined between two infinitesimally close surfaces at low Reynolds numbers. When height-averaged, the velocity field can be considered irrotational and thus a special form of quasi two-dimensional potential flow mathematically analogous to electrostatic fields or, perhaps more precisely, to current flowing in a thin conducting plate (see Table 1).

$$\mathbf{v}(x,y) = -\frac{G^2}{12\eta}\nabla p(x,y). \tag{1}$$

Thus the velocity profile linearly depends on the gradient of the hydrostatic pressure profile *p(x,y)* inside the flow under the probe, with a proportionality constant depending both on gap size *G* and viscosity η. Therefore, Gauss's law can also readily be applied to describe velocity field lines under a microfluidic probe. Around a single round aperture of dimension *a* and flow rate Q_i, located at position $\mathbf{r_i}$' from the origin, the velocity profile at a position **r** from the origin is given by

$$\mathbf{v_i} = \frac{Q_i}{2\pi G}\frac{\mathbf{r}-\mathbf{r_i'}}{|\mathbf{r}-\mathbf{r_i'}|^2}. \tag{2}$$

For $|r\text{-}r'| > a/2$ (the aperture radius), the flow extends radially outward from the source and decreases as 1/r as it extends to infinity, just like the electric field around a thin infinite charged rod. The relationship described in (2) will also correctly describe flow outside a square aperture of side length *a* for $|r\text{-}r'| >> a/2$. To compute flow in a more complex object, we next apply the superposition principle. For example, two point sources of flow rate $Q_{asp} = \alpha\, Q_{inj}$ located at $\mathbf{r_i}' = (\pm d/2,0)$ from the center of the probe produce a flow dipole, while two orthogonal pairs of point sources with the same flow rate ratio α located at $\mathbf{r_i}' = \{(\pm d/2,0), (0,\pm d/2)\}$ constitute a flow quadrupole (see *Fig. 1 CD*). Thus, expressing vectors using their cartesian components, we obtain

$$\mathbf{v} = \frac{Q_{inj}}{2\pi G}\left(\frac{(x-d/2)\hat{\mathbf{x}}+y\hat{\mathbf{y}}}{(x-d/2)^2+y^2} - \alpha\frac{(x+d/2)\hat{\mathbf{x}}+y\hat{\mathbf{y}}}{(x+d/2)^2+y^2}\right) \tag{3}$$

representing flow beneath a MFP anywhere except inside the apertures of dimension *a*. The x and y axis are introduced earlier in Fig. 1CD. The flow profile for the MQ has been reported elsewhere [8].

B. Determination of stagnation points and HFC dimensions

The complete expression of **v**(x,y) underneath a probe arising from a superposition of sources is rather unwieldy. Yet we can extract useful information on the HFC dimensions by looking at the stagnation points. In both MFP

and MQ, the stagnation points represent the furthest point from the device's center a non-diffusive injected species can travel (Fig. 1CD). In the particular case of the MQ, another stagnation point exists at the very center of the probe (at **r** = (0,0)) where the two injected streams meet and diverge toward the aspiration apertures. Since they are located on the X-axis, these points satisfy the condition

$$v_x(R,0) = 0, \tag{4}$$

where R≡ X_{SP} is the location of the outer stagnation point (see Fig. 1C-D). For both the MFP and the MQ (result described in [8]), the condition from (3) applied on (2) yields:

$$R_{MFP}(\alpha) = \frac{d}{2}\frac{\alpha+1}{\alpha-1}, \qquad R_{MQ}(\alpha) = \pm\frac{d}{2}\sqrt{\frac{\alpha+1}{\alpha-1}}. \tag{5}$$

Where α is the ratio of aspiration to injection flow rates, and d is center-to-center distance between two opposite apertures (see Fig. 1C-D). Similarly, the probe half width $W/2$ (in the y direction) can be numerically identified as the point satisfying the condition

$$v_y(x, W/2) = 0. \tag{6}$$

C. Controlling probe operation using HFC dimensions

Precisely controlling the values of R and W/2 have important consequences when operating the probe in surface processing mode as these parameters correspond to the dimensions of the probe's writing tip, just like the dimensions of a brush determine the size of a trait (Fig. 3). When moved parallel to the dipole axis, the probe will draw a regular line of width $W_{//} = W(\alpha)$. When moved in a direction perpendicular to the dipole axis, the width of the trait will be given by

$$W_\perp = d/2 + R_{MFP}(\alpha) = \frac{\alpha d}{\alpha - 1}. \tag{7}$$

A similar analysis can be carried out using the general shape of the quadrupole to provide an effective brush stroke in surface patterning mode. We obtain, for the MQ,

$$W_{//} = d, W_\perp = cR_{MQ}(\alpha) = \tfrac{cd}{2}\sqrt{\tfrac{\alpha+1}{\alpha-1}}. \tag{8}$$

The constant c in (8) has value of either c = 1, when reagent is injected only through one of the two injection apertures (as in Fig. 1F), or c = 2, when reagent is injected in both. Values found in (8) and (9) represent the maximum and minimum possible brush stroke using both probe types. Any value in between can be achieved by rotating the probe's dipole axis by an angle θ with respect to the writing direction. Using a simple projection, the effective width of the brush trait can therefore be calculated as:

$$W_{eff}(\alpha) = W_{//}(\alpha)cos\theta + W_\perp(\alpha)sin\theta. \tag{9}$$

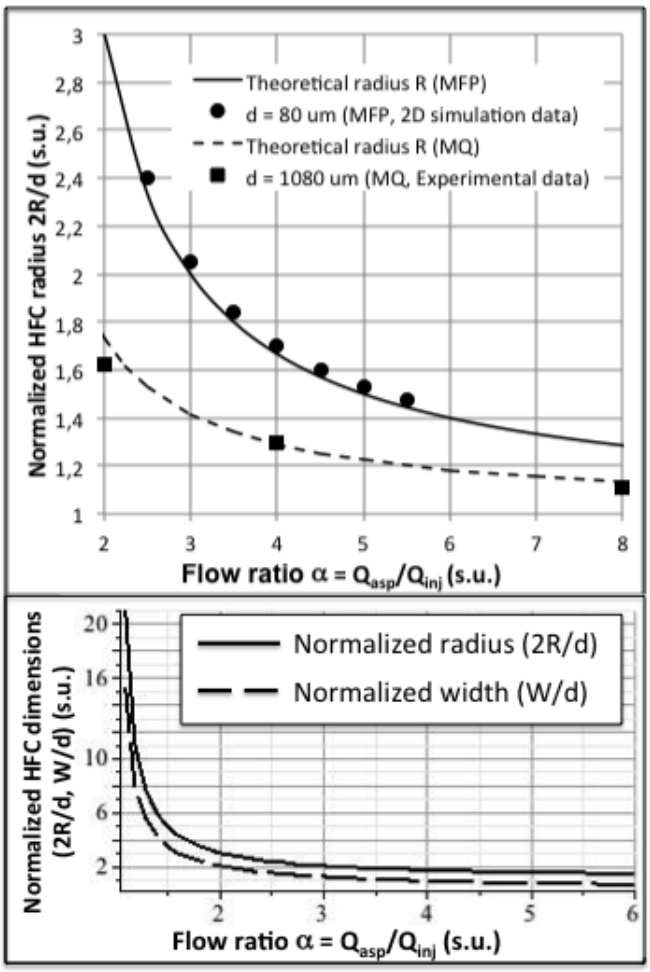

Figure 2. Analysis of the HFC area of a MFP. A) Plot of simulated and experimental values for the normalized probe radius *2R/d* as a function of alpha for both the MFP and MQ. Simulations results for the MFP were produced using a 2D probe model in COMSOL. Experimental results were obtained from [8]. B) Comparison between the scaling of probe radius R (analytical result) and normalized probe half width *2W/2d = W/d* (obtained numerically).

III. RESULTS

Analytical models have been compared with experimental data (MQ) and numerical simulations using COMSOL (MFP). Fig. 2A describes the relationship between (5) and numerical and experimental results. This key result describes the extent of the hydrodynamic flow confinement (HFC) zone located directly underneath the probe. Thus the outer stagnation points in multipolar probes represent the furthest

points from the probe center that a non-diffusive species can reach. Experimental and numerical results provide an excellent match with the analytical model when $d >> a$. Computed numerical values for probe width as a function of α (Fig. 2B) also reveal a similar scaling for probe width. Thus we can infer that the HFC area scales with $\sim R^2$ (i.e. $\sim d^2$). As HFC area is in fact the area of the probe's writing tip, controlling the probe's flow rate ratio α will ensure a precise brush stroke when using a probe in writing mode.

It is important to point out that the effective shape of the stroke described in (9) does not take into account the diffusive broadening of the reagent used in the probe, which will vary with the Péclet number as $Pe^{-1/2}$ [8]. Thus, it should closely match experiment for low diffusivity reagents, such as large molecules (IgG, Ab, DNA) but should underestimate its value for smaller molecules (fluorescein, trypsin, cytokines, etc.) as they display higher diffusivities. Furthermore, we neglect the effect of probe displacement on the shape of the HFC, which is valid only for slow displacements of the probe relative to the velocity profile inside the HFC.

IV. Conclusion

We have provided in this paper a simple analytical framework to analyze HFC with both MFPs and MQs simultaneously. The analysis readily provides scaling laws to control HFC radius *R*. Numerical simulations clearly confirmed the exactness of the results and further showed that the HFC width *W* scaled in a similar fashion.

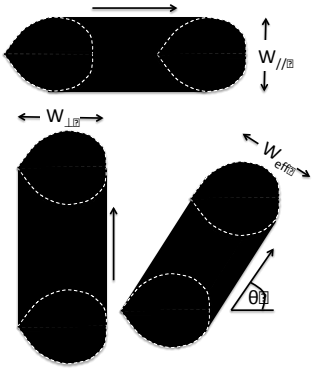

Figure 3. Various brush strokes achievable with a MFP in surface patterning mode. Maximum width is $W_{\perp}$, minimum width is $W_{//}$. Any intermediary value can be obtained by rotating the probe dipole axis by an angle α with respect to the direction of movement.

It is of interest to note that, in general, HFC dimensions can be strictly determined using four user-controlled parameters, including two design parameters: interaperture distance *d* of the probe and aperture dimension *a*, and two user operation parameters: aspiration to injection flow rate ratio $\alpha = Q_{asp}/Q_{inj}$, and the vertical gap *G* between probe and surface. When the gap *G* is sufficiently small to meet Hele-Shaw conditions ($G^2 << d^2$) and the aperture size is sufficiently small with respect to probe size (a << d), the HFC dependence is further reduced to only two parameters, α and *d*. As long as the Reynolds number beneath the probe is much smaller than unity (Stokes Flow regime), the absolute value of either injection or aspiration flow rate is also irrelevant to HFC dimensions, with the flow ratio α being the key driving parameter.

Based on these observations we go on to describe the possible "brush strokes" that can be performed using a MFP or an MQ in surface patterning mode. The simple results provided can be used to control the stroke's width and length by varying flow ratio α and planning the appropriate probe design by selecting values of interaperture distance *d* and aperture size *a* in an appropriate range for the planned experiment.

Acknowledgment

The authors wish to acknowledge support from FRQ-NT and NSERC. M.S. thanks support from FRQ-NT scholarship and ISS NSERC-CREATE fellowship. M.A.Q. acknowledges a Alexander Graham Bell Canada Graduate NSERC Scholarship and, D.J. acknowledges support from a Canada Research Chair. We thank Farhang Tarlan for carrying out several numerical simulations, and Roozbeh Safavieh for insightful discussions.

References

[1] E. K. Sackmann, A. L. Fulton, and D. J. Beebe, "The present and future role of microfluidics in biomedical research.," *Nature*, vol. 507, no. 7491, pp. 181–9, Mar. 2014.

[2] G. V Kaigala, R. D. Lovchik, and E. Delamarche, "Microfluidics in the 'open space' for performing localized chemistry on biological interfaces.," *Angew. Chem. Int. Ed. Engl.*, vol. 51, no. 45, pp. 11224–40, Nov. 2012.

[3] M. A. Qasaimeh, S. G. Ricoult, and D. Juncker, "Microfluidic probes for use in life sciences and medicine.," *Lab Chip*, vol. 13, no. 1, pp. 40–50, Jan. 2013.

[4] D. Juncker, H. Schmid, and E. Delamarche, "Multipurpose microfluidic probe.," *Nat. Mater.*, vol. 4, no. 8, pp. 622–8, Aug. 2005.

[5] R. D. Lovchik, G. V Kaigala, M. Georgiadis, and E. Delamarche, "Micro-immunohistochemistry using a microfluidic probe.," *Lab Chip*, vol. 12, no. 6, pp. 1040–3, Mar. 2012.

[6] A. Queval, N. R. Ghattamaneni, C. M. Perrault, R. Gill, M. Mirzaei, R. A. McKinney, and D. Juncker, "Chamber and microfluidic probe for microperfusion of organotypic brain slices.," *Lab Chip*, vol. 10, no. 3, pp. 326–34, Feb. 2010.

[7] A. Sarkar, S. Kolitz, D. A. Lauffenburger, and J. Han, "Microfluidic probe for single-cell analysis in adherent tissue culture.," *Nat. Commun.*, vol. 5, p. 3421, Jan. 2014.

[8] M. A. Qasaimeh, T. Gervais, and D. Juncker, "Microfluidic quadrupole and floating concentration gradient.," *Nat. Commun.*, vol. 2, no. May, p. 464, Jan. 2011.

[9] M. A. Qasaimeh, M. Astolfi, S. Pyzik, S. Vidal, and D. Juncker, "Neutrophils migrate longer distances in moving microfluidic concentration gradients compared to static ones," in *The 17th International Conference on Miniaturized Systems for Chemistry and Life Sciences (microTAS)*, 2013, pp. 2007–2009.

[10] G. K. Batchelor, *An introduction to fluid dynamics*. Cambridge University Press, 2000.

[11] K. V Christ and K. T. Turner, "Design of hydrodynamically confined microfluidics: controlling flow envelope and pressure.," *Lab Chip*, vol. 11, no. 8, pp. 1491–501, Apr. 2011.